Study of the "Fast SCR" -like mechanism of H2-assisted SCR of NOx with ammonia over Ag/Al2O3

Doronkin, Dmitry E.; Fogel, Sebastian; Tamm, Stefanie; Olsson, Louise; Khan, Tuhin Suvra; Bligaard, Thomas; Gabrielsson, Pär; Dahl, Søren

Published in:
Applied Catalysis B: Environmental

Link to article, DOI:
10.1016/j.apcatb.2011.11.042

Publication date:
2012

Study of the "Fast SCR"-like mechanism of H_2-assisted SCR of NO_x with ammonia over Ag/Al_2O_3

Dmitry E. Doronkin[1], Sebastian Fogel[2], Stefanie Tamm[3,4], Louise Olsson[3,4], Tuhin Khan[5], Thomas Bligaard[6], Pär Gabrielsson[2], Søren Dahl[1]*

[1]Center for Individual Nanoparticle Functionality (CINF), Department of Physics, Technical University of Denmark, Fysikvej 307, 2800 Kgs. Lyngby, Denmark

[2]Haldor Topsøe A/S, Nymøllevej 55, 2800 Kgs. Lyngby, Denmark

[3]Competence Center for Catalysis, Chalmers University of Technology, SE-412 96 Göteborg, Sweden

[4]Chemical Reaction Engineering, Chalmers University of Technology, SE-412 96 Göteborg, Sweden

[5]Center for Atomic-scale Materials Design (CAMD), Department of Physics, Technical University of Denmark, Fysikvej 307, 2800 Kgs. Lyngby, Denmark

[6]SUNCAT Center for Interface Science & Catalysis, SLAC National Accelerator Laboratory, Menlo Park, CA 94025, U.S.A.

* Corresponding author: tel.: +45-4525-3275, e-mail: *dmdo@fysik.dtu.dk*

Abstract. It is shown that Ag/Al_2O_3 is a unique catalytic system for H_2-assisted selective catalytic reduction of NO_x by NH_3 (NH_3-SCR) with both Ag and alumina being necessary components of the catalyst. The ability of Ag/Al_2O_3 and pure Al_2O_3 to catalyse SCR of mixtures of NO and NO_2 by ammonia is demonstrated, the surface species occurring discussed, and a "Fast SCR"-like mechanism of the process is proposed. The possibility of catalyst surface blocking by adsorbed NO_x and the

influence of hydrogen on desorption of NO_x were evaluated by FTIR and DFT calculations.

Keywords: Ag/Al_2O_3; alumina; NO_x SCR; Fast SCR; FTIR

1. Introduction

Nitrogen oxides (NO_x) are the most challenging pollutant to address for light-duty diesel vehicles and sophisticated techniques like advanced fuel injection, exhaust gas recirculation (EGR), turbocharging etc., are used by engine manufactures to reduce emissions. But, NO_x removal by exhaust aftertreatment is still required due to stricter emmision regulations and the trade off between fuel consumption and NO_x emmision, *i.e.*, the price for reducing fuel consumption and CO_2 emission by ~ 15% equals to ~ 50% increase in NO_x emissions [1].

Selective catalytic reduction (SCR) is the leading NO_x control technique with ammonia as a reductant. Commonly used catalysts are vanadia-based catalysts, Cu and Fe-containing zeolites. However, none of the systems demonstrates high thermal durability together with a good activity throughout a broad temperature region from 150 to 550 °C [1]. This fact explains the reason for the on-going research of novel catalytic systems for NH_3-SCR, which are supposed to be non-toxic, inexpensive and durable.

Alumina supported metals, such as Ag, In, Sn etc. [2,3,4,5] are known to catalyse NO_x SCR by hydrocarbons under the conditions of lean-burn engine exhaust. The major drawback of these catalytic systems is their very poor activity at low temperatures. It has been found that addition of hydrogen to the gas feed can substantially improve the low-temperature activity of Ag/Al_2O_3 [6,7,8]. Interestingly, several groups have also demonstrated the possibility of Ag/Al_2O_3 to facilitate SCR of NO_x by ammonia or urea

with co-feeding hydrogen, resulting in nearly 90% NO_x conversion at temperatures as low as 200 °C [9,10].

Hydrogen for this reaction can be provided on board of the vehicule by two means depending on the used reductant. The required amount of hydrogen can be produced in an on-board fuel reformer without the necessity to change the existing fuel infrastructure. This is convenient for hydrocarbon SCR systems utilizing Ag/Al_2O_3 catalysts and currently leads to fuel penalties from 5 to 10% [11, 12] which might be improved by the optimization of the system. For the NH_3 SCR applications hydrogen can be produced by cracking of part of the ammonia. Pure NH_3 required for this purpose can be stored on board in form of solid metal ammine salts [13]. The suggested system allows accurate and independent dosing of ammonia to the SCR catalyst and to the cracker where it can be decomposed to form the required hydrogen. Using ammonia for hydrogen storage has earlier been suggested for fuel cell applications but can also be applied for NO_x SCR applications [14, 15].

There is no general agreement about the necessary concentration of hydrogen for the effective reduction of NO_x by ammonia over Ag/Al_2O_3. One can find H_2:NO_x ratios varying from 5 to 10 in the literature [9, 10, 16-18] which is a rather high value. However Shimizu and Satsuma have demonstrated ever increasing NO_x reduction rate in the interval of H_2:NO_x ratios from 0 to 50 [17] which makes the choice of H_2 concentration a matter of finding the optimum between the amount of ammonia spent on hydrogen production and the SCR efficiency. We are considering a H_2:NO_x ratio 2.4 as an optimum in this work.

Hydrogen has also been considered as the only reductant in H_2-SCR of NO_x, however currently available catalysts allow effective removal of NO_x only when using

H_2:NO_x > 10 and such amount of hydrogen cannot be produced on board at an affordable price [19-21].

In this work we studied several catalysts: Ag supported on different carriers (γ-Al_2O_3, TiO_2 and ZrO_2), Sn and In supported on γ-Al_2O_3 and pure alumina under the conditions of H_2-assisted SCR of NO_x with NH_3. The aim of this study is to investigate the possibility of replacing traditional NO_x SCR catalysts by Ag/Al_2O_3 thus obtaining high catalyst activity even at low temperatures. Another goal of the study is to give insight to the mechanistic aspects of H_2-assisted NO_x SCR by ammonia.

2. Experimental

2.1. Catalyst preparation

Parent γ-alumina (Puralox SCFa-140, 59 ppm Fe_2O_3 content) was kindly provided by SASOL. Prior to its study as a catalyst it was calcined at 550 °C for 4 hours in static air.

1%Ag/Al_2O_3, 3%Sn/Al_2O_3 and 3%In/Al_2O_3 were obtained by incipient wetness impregnation of parent γ-alumina by corresponding amounts of $AgNO_3$, $SnCl_4 \cdot 5H_2O$ and $InCl_3 \cdot 4H_2O$ (all from Sigma-Aldrich) solutions in deionized water. 1%Ag/TiO_2 and 1%Ag/ZrO_2 were obtained by incipient wetness impregnation of TiO_2 (anatase containing 10%SiO_2) and ZrO_2 (E10, Magnesium Elektron Ltd.) by the aqueous solution of $AgNO_3$. After impregnation all catalysts were dried at room temperature overnight and calcined at 550 °C for 4 hours in static air.

The calcined catalysts were pressed, crushed and sieved to obtain the fraction 0.18 – 0.35 mm (mesh 80 – mesh 45).

2.2. TEM measurements

TEM measurements were carried out in a TECNAI T20 transmission electron microscope equipped with an Oxford Instruments EDX detector. For the measurements the catalyst powder (in a dry form) was dispersed on a copper TEM grid covered with a lacey carbon film. Images were acquired using DigitalMicrograph from Gatan Inc.

2.3. Catalytic studies

The catalytic measurements were carried out in a fixed-bed quartz flow reactor (inner diameter = 4 mm) in a temperature programmed mode while the temperature was decreased from 400 °C to 150 °C with a rate 2 °C/min. The temperature was controlled using an Eurotherm 2416 temperature controller with a K-type thermocouple. 45 mg of catalyst was diluted with 100 mg of SiC (mesh 60) and placed on a quartz wool bed. The bed height was ~11mm and the GHSV, calculated using the volume of the pure catalyst was ~ 110,000 h^{-1}. The gas composition normally contained 500 ppm NO, 520 ppm NH_3, 8.3% O_2, and 7% water balanced with Ar. During some tests 1200 ppm of H_2 was added to the gas feed. The gas feed was mixed from 2000 ppm NO in Ar, 2000 ppm NH_3 in Ar, 4000 ppm H_2 in Ar (Air Liquide), oxygen and argon (AGA), dosed by individual mass flow controllers (UNIT Celerity). Water was dosed by an ISCO 100DM syringe pump through a heated capillary. Mixtures of NO and NO_2 were obtained by feeding NO and oxygen through a long capillary, giving NO_x with 26 – 47% NO_2. Reaction products were analyzed by a Thermo Fisher Nicolet 6700 FTIR analyzer, equipped with a gas cell (2 m optical pathlength). Gas capillaries were heated to ~130 °C and the FTIR gas cell to 165 °C to avoid condensation of water and formation of ammonium nitrate. To simplify experimental procedure we are not using CO_2 in the

study as we have not observed CO_2 effect on the NO_x SCR by NH_3 during the preliminary experiments with Ag/Al_2O_3 catalysts.

Conversions were calculated using the following equations:

$$X_{NOx} = 1 - \frac{C_{NOx}^{outlet}}{C_{NOx}^{inlet}} \quad (1)$$

where X_{NOx} denotes total conversion of NO_x and $C_{NOx}{}^{inlet}$ and $C_{NOx}{}^{outlet}$ is the NO_x concentrations on the inlet and outlet of the reactor, where:

$$C_{NOx} = C_{NO} + C_{NO_2}. \quad (2)$$

NH_3 conversion (total), NH_3 conversion to NO_x (when no NO_x is fed) and NO conversion to NO_2 (when no NH_3 was fed) were calculated correspondingly:

$$X_{NH_3} = 1 - \frac{C_{NH_3}^{outlet}}{C_{NH_3}^{inlet}}, \quad (3)$$

$$X_{NH_3 \to NOx} = \frac{C_{NOx}^{outlet}}{C_{NH_3}^{inlet}}, \quad (4)$$

$$X_{NO \to NO_2} = \frac{C_{NO_2}^{outlet}}{C_{NO}^{inlet}}, \quad (5)$$

and the ratio of converted NO to converted NO_2 in the experiments with NO and NO_2 mixtures:

$$\frac{C_{NO}^{conv.}}{C_{NO_2}^{conv.}} = \frac{C_{NO}^{inlet} - C_{NO}^{outlet}}{C_{NO_2}^{inlet} - C_{NO_2}^{outlet}}. \quad (6)$$

NH_3:NO_x conversion ratio below 400 °C was always 1:0.95-1.05 for all tested catalysts, therefore we are presenting only NO_x conversion values in the discussion.

2.4 DRIFTS studies

In-situ diffuse reflectance infrared Fourier transform spectroscopy (DRIFTS) experiments were performed using a BioRad FTS 6000 FTIR spectrometer equipped with a high-temperature reaction cell (Harrick Scientific, Praying Mantis) with KBr windows. The temperature of the reaction cell was controlled with a K-type thermocouple connected to a Eurotherm 2416 temperature controller. Gases were introduced into the reaction cell via individual mass flow controllers (Bronkhorst Hi-Tech). The gas composition at the outlet of the DRIFTS cell was analyzed by a mass spectrometer (Balzers QuadStar 420).

Each experiment was performed using approximately 100 mg of γ-Al_2O_3 powder, using new powder for each experiment. The powder was initially pretreated in a flow of 8 % O_2 in Ar at 500 °C for 30 min, subsequently a background spectrum (60 scans, resolution 2 cm^{-1} at 4000 cm^{-1}) was recorded in a flow of Ar. At 500 °C, 185 ppm NO_2, 315 ppm NO, 520 ppm NH_3 and 8.3% O_2 were added to the feed. Then the catalyst was cooled with a ramp rate of 10 °C/min in the reaction mixture to reaction temperature, where the temperature is held for 10 min for stabilization. Subsequently, NH_3 is removed from the feed gas mixture for 30 min and added again to it for 10 min. This procedure was repeated once. Thereafter, 1250 ppm H_2 were added for 10 min to the feed gas and, subsequently, NH_3 was removed again. The evolution of absorption bands in the spectra was followed using the kinetic mode (9 scans/spectrum, 6 spectra/min,) at a resolution of 2 cm^{-1} at 4000 cm^{-1}. The data are presented as absorbance, which is defined as the logarithm of the inverse reflectance (log 1/R). All DRIFTS experiments were carried out using a total flow rate of 100 ml/min which corresponds to a space velocity of about 62 000 h^{-1}.

2.5. DFT Calculations

Plane wave DFT code DACAPO is used to calculate the adsorption energies and the gas phase energies of the adsorbates. Plane wave cutoff of 340.15 eV and density cutoff of 680 eV are used for the calculations. The core electrons are described by the Vanderbilt ultrasoft pseudopotential [22]. RBPE is used as the exchange correlation energy function [23]. Fermi population of the Kohn-Sham states is $k_bT = 0.1$ eV. The convergence limit is set as maximum change in force constant $f_{max} = 0.03$ eV.

The adsorption energies of O, NO, NO_2 and NO_3 are studied over six different transition metals (Ag, Cu, Pd, Pt, Rh, Ru) on both the (111) terrace and the (211) step surfaces. We use a 2×2 surface cell for O and NO for (111) terrace, 2×1 surface cell for O and NO for (211) step surface, 3×3 surface cell for NO_2 and NO_3 adsorption study on (111) terrace and the 3×1 surface cell for NO_2 and NO_3 adsorption study (211) step surfaces, with 8 × 8 × 1 Monkhorst-Pack **k**-point sampling in the irreducible Brillouin zone for all the 2×2 surface cells, 8 × 6 × 1 Monkhorst-Pack **k**-point sampling in the irreducible Brillouin zone for all the 2×1 surface cells and 4 × 4 × 1 Monkhorst-Pack **k**-point sampling for both 3×3 and 3×1 surface cells. For all the (111) surfaces we use a four-layer slab where the two topmost layers are allowed to relax whereas for the (211) surfaces with 2×1 surface cell we use a slab model with twelve layers where the topmost six layers are allowed to relax and for (211) surfaces with 3×1 surface cell we use a slab model with nine layers where the topmost three layers are allowed to relax.

For the calculation of γ-Al_2O_3 and the adsorption of different species on γ-Al_2O_3 we also used the DACAPO code with a plane wave cutoff of 340.15 eV and a density cutoff of 680 eV. A 4× 4 × 1 Monkhorst-Pack **k**-point sampling in the irreducible Brillouin zone was used for γ-Al_2O_3. The γ-Al_2O_3 surface was modeled by a step on a

nonspinel γ-Al_2O_3 structure which was derived bulk γ-Al_2O_3 model [24]. The cell parameters for the γ-Al_2O_3 step closed packed surface are a = 8.0680 Å and b = 10.0092 Å and α = β = γ = 90˚. For the γ-Al_2O_3 surface the bottom two layers were fixed where as the top three layers were allowed to relax.

In all the model surfaces, the neighboring slabs are separated by more than 10 Å of vacuum.

NO_x and HNO_x adsorption energies were calculated relative to gas phase zero energy points of these species.

The energy minimum adsorption geometries used in the calculations are presented in the supplementary material.

3. Results and discussion

3.1. Unique activity of Ag/Al_2O_3 in H_2-assisted NH_3-deNO_x

NO_x conversions obtained over the prepared catalysts at 380 °C tested under the conditions of SCR of NO_x with NH_3, without and with H_2 in the exhaust, are given in Table 1. In the absence of H_2 all the catalysts are inert with respect to NO_x reduction or ammonia oxidation at temperatures below 400 °C. The hydrogen effect was observed only for Ag/Al_2O_3, Ag/TiO_2 and In/Al_2O_3 (Fig. 1). The former catalyst demonstrates extremely high performance with NO_x conversion exceeding 80% at 200 °C at GHSV = 110 000 h^{-1}. No more than 5 ppm N_2O was observed in the products. Ag/TiO_2 is much less active with maximum NO_x conversion of 25% at 380°C. The activity of In/Al_2O_3 below 400 °C is only marginal. Therefore only Ag/Al_2O_3 may be considered for practical applications among the tested catalysts. Futhermore, it is evident that both silver and alumina are nesessary components of the catalyst to obtain a high

performance in deNO$_x$. Removal or change of each of these components lead to almost inactive catalysts. Therefore, it is likely that both silver and alumina take part in the catalytic cycle or the active site is positioned on the interface between Ag and Al_2O_3.

3.1.1. TEM data on Ag/Al_2O_3 and Ag/TiO_2

In order to clarify if it is the catalyst morphology that determines the drastic difference in the SCR performance of Ag/Al_2O_3 and Ag/TiO_2, TEM images of the samples were obtained. These micrographs are compared in Fig. 2. The choice of the catalysts in question is dictated by their common properties (Ag loading, BET surface area of the support, preparation technique), which is in contrast to their very different catalytic activity.

EDX shows the presence of ~1% Ag in the both depicted catalyst grains. However, we were unable to locate any metal particles with diameters larger than 2-3nm in both catalyst samples. This confirms a high dispersion of Ag in both Ag/Al_2O_3 and Ag/TiO_2 catalysts, which might be in the form of clusters of 4-8 Ag atoms as suggested by Kondratenko et al. [16]. Therefore the large difference in SCR activity of Ag/Al_2O_3 and Ag/TiO_2 is not due to a large difference in Ag dispersion.

3.2. Study of the mechanism of H_2-assisted NH_3-deNO$_x$

3.2.1. Experiments with Ag/Al_2O_3 where components of the feed are omitted

Studies of the mechanism of hydrogen-assisted NO$_x$ SCR by NH_3 on Ag/Al_2O_3 were already performed before [16, 17], where the attention was drawn to the state of silver. Our catalytic experiments show a uniqueness of the Ag/Al_2O_3 catalytic system, in which both components play a vital role.

To have a notion of the individual reactions occuring during NO_x SCR by NH_3 we consequtively run catalytic tests with one of the components absent in the feed.

According to the results obtained so far it is already clear that the removal of hydrogen leads to a completely inactive catalyst with regards to NH_3-deNO_x (Table 1) or ammonia oxidation. The concentration of all monitored gases remained constant during temperature ramping from 400 to 100 °C when no H_2 was in the feed. The same is true for the removal of oxygen from the feed – no NO reduction or NH_3 oxidation was observed without O_2.

When NH_3 was removed from the gas feed, a pronounced oxidation of NO to NO_2 starting from 100 °C was observed (fig. 3, solid line). Together with that a very low NO_x to N_2 conversion (dotted line, max. 4%) was observed indicating that hydrogen normally acts not as the main reductant but as a co-reductant. When both ammonia and hydrogen were removed from the feed, no oxidation of NO to NO_2 was observed.

The latter observation agrees with the data obtained in [6, 16]. As suggested in [6], hydrogen addition promotes oxidation of NO. However, we observed no oxidation of NO to NO_2 during the experiments with Ag/TiO_2 and Ag/ZrO_2 catalysts. This shows once again that not only Ag, but also the support plays an important role in the catalytic activity of Ag/Al_2O_3 which also agrees with the data on C_3H_8-SCR reported in [6].

The mechanism of O_2 activation by hydrogen has been suggested earlier [25, 26] as follows. On the first step hydrogen dissociates on active Ag_n+ sites on alumina to form an acidic proton and hydride Ag_n–H. This hydride later reacts with oxygen to form a reactive oxidant, such as hydroperoxy radicals (HO_2), peroxide (O_2^{2-}), or superoxide ions (O_2^-) all of which later oxidize NO to NO_2.

When removing NO from the NO, NH_3, H_2, O_2 and H_2O containing feed, NH_3 oxidation to N_2 (fig. 4, solid line) and to NO_x (fig. 4, dotted line) occurs at temperatures higher than 200 °C. Comparison of the data in fig. 3 and fig. 4 suggests that NO oxidative acivation starts at significantly lower temperature (corresponding to the NH_3-deNO_x light-off temperature) than NH_3 oxidative activation. Therefore it is more likely that oxidative activation of NO is an important step in the overall catalytic mechanism of NO_x SCR over Ag/Al_2O_3.

The data does not support a hypothesis of oxidative dehydrogenation of NH_3 (or NH_3-assisted NO decomposition) being the main catalysed step of H_2-assisted NH_3-deNO_x over Ag/Al_2O_3 [18]. Ag/Al_2O_3 rather participates in NO activation and possibly in the reaction of NH_3 with NO_x intermediates [16].

The hydrogen promoted oxidative activation of NO has been already reported by Satokawa et al. for NO_x SCR by C_3H_8 [6]. However in that study oxidative activation of NO was not enough to initiate SCR and activation of C_3H_8 by H_2 has been reported to be necessary which makes it different from SCR by NH_3.

3.2.2. Experiments with feeding NO and NO_2 mixtures over Ag/Al_2O_3 and Ag/ZrO_2

After realizing that the hydrogen promoted oxidation of NO to NO_2 may be the first step in the H_2-assisted NH_3-deNO_x we decided to do catalytic tests with a feed containing a mixture of NO and NO_2 as NO_x. Since H_2 facilitates reversible NO-NO_2 tranformation, undesirable for these experimens, no H_2 was co-fed.

Fig. 5 shows NO_x conversions to N_2 obtained over Ag/Al_2O_3 when a NO and NO_2 mixture is fed as NO_x (containing 26, 34 and 47% NO_2) and over Ag/ZrO_2 with 34% NO_2 in NO as NO_x. Surprisingly for all three cases we observe nearly equal, maximum

30%, NO_x conversion which changes only slightly with temperature. NH_3 conversion profiles follow the NO_x conversion profiles and they are therefore not shown. This observation allows us to conclude that oxidation of NO to NO_2 over Ag/Al_2O_3, at least, partially accounts for the activity of this catalyst in the NO_x SCR. This agrees with previous works, evidencing oxidation of NO to NO_2 involving H_2 [25] and supposing it to be crucial for low-temperature NO_x SCR by hydrocarbons [27].

Moreover, SCR of the NO and NO_2 mixture by NH_3 is not a unique feature of Ag/Al_2O_3 but was also observed for other supports though to a less extent, e.g. with 15% maximum NO_x conversion in the case of Ag/ZrO_2 (see Fig. 5, gray dotted line). Thus metal oxides other than alumina can catalyse NO+NO_2 SCR by NH_3 but Ag/Al_2O_3 with H_2 co-feeding is required to oxidize NO at low temperatures. Therefore, we are focusing our study on Ag/Al_2O_3 catalysts and the corresponding alumina support.

The effect of increasing the NO_x SCR rate by feeding NO and NO_2 mixture has already been noticed for other catalytic systems including vanadia-based catalysts [28] and zeolites [29]. The effect is called "Fast-SCR" and characterized by a well-defined stoichiometry of NO:NO_2 being 1:1.

To check if the NO:NO_2 conversion without H_2 in the feed can be ascribed to "Fast SCR" [29], we calculated the ratio of consumed NO to consumed NO_2 (Fig. 6). In our case the ratio of consumed NO to consumed NO_2 changed with temperature from negative values (only NO_2 is consumed and a small amount of NO is produced from it) to positive values up to 1 in case of feeding 26% NO_2 (Fig. 6). Interestingly, the temperature at which NO starts to be consumed (~ 150 °C) coincides with the onset temperature of H_2-assisted SCR (Fig. 1). Therefore we can suppose that parts of the mechanisms of both H_2-assisted NO SCR by NH_3 and NO+NO_2 SCR by NH_3 are

similar. But in case of NO+NO_2 SCR we observed a conversion limit at ~30%, when almost 100% conversion is obtained in H_2-assisted NO_x-SCR. This could be explained by blocking of the catalyst surface by adsorbed nitrate species [25]. The poisoning effect of surface nitrates for propane-SCR was observed in [26], where the authors also demonstrated the ability of hydrogen to effectively remove adsorbed nitrate species. Thus, introduction of hydrogen may facilitate not only NO to NO_2 conversion, but also regeneration of the catalyst surface, which removes the 30% conversion limit.

In general, the ratio of converted NO to converted NO_2 depends on the total amount of NO_2 in the feed and decreases with increase in NO_2 content. The higher the NO_2 content – the larger is the part of NO_2 in the NO_x that is converted to N_2. Independent on this, the ratio of converted NO_x to converted NH_3 was always 1:1 and maximum conversion remained constant at ~30%.

3.2.3. Experiments with feeding NO and NO_2 mixtures over pure γ-Al_2O_3

In some of the papers on H_2-assisted NO SCR by NH_3, published earlier [16, 17], alumina was considered only as a support for the active Ag nanoparticles. In this case, the properties of alumina could influence the catalyst activity indirectly by tuning the Ag particle size and distribution. In the following we test this assumption.

With or without hydrogen γ-alumina stays inactive under the experimental conditions of NO_x SCR by ammonia when NO is the only component of NO_x in the feed. This changes when NO_2 is introduced. Fig. 7 shows a comparison of NO_x (26% NO_2 of total NO_x at the reactor inlet) conversion by NH_3 obtained over pure Al_2O_3 (solid line) and Ag/Al_2O_3 (dotted line) with no H_2 in the feed. The profiles are almost identical indicating that presence of Ag in the catalyst is important only for the H_2-

assisted reaction. Taking into account the overall quantity of NO_2, which can be produced from NO in presence of H_2 over Ag/Al_2O_3 (Fig.3), it is evident that alumina can significantly contribute to the overall H_2-assisted NO SCR mechanism. Thus, it cannot be neglected that alumina is an active part of the catalyst. Moreover the stoichiometry of $NO+NO_2$ SCR conversion over alumina follows the same trend as for the Ag/Al_2O_3 (Fig. 8), which may demonstrate the same mechanism is working in both cases. Running $NO+NO_2$ SCR with H_2 in the feed over pure Al_2O_3 yield almost the same NO_x conversion as as for the test without H_2 (Fig.7, solid line).

Thus the presence of Ag and H_2 is mostly important for oxidative activation of NO and possibly removal of adsorbed species blocking the catalyst surface. The reaction of NO and NH_3 with the obtained NO_2 can proceed further over pure Al_2O_3 yielding N_2. This result agrees with the results of J. Lee et al. [30], who demonstrated the ability of pure alumina to catalyse the reduction of NO, activated over Ag/Al_2O_3, by partially oxidized hydrocarbons. At the same time, Meunier and Ross [31] observed the ability of pure alumina to run the propene SCR of NO_2 (but not of NO).

From the analysis of the stoichiometry of the $NO+NO_2$ SCR reaction (Figs. 6 and 8) it can be concluded that at temperatures lower than 150°C only NO_2 reacts with NH_3. The production of NO from NO_2 can also be observed, which is thermodynamically not possible and is likely due to an uncomplete SCR reaction between NO_2 and NH_3. Above 350 °C NO_2 decomposition to NO is thermodinamically favorable, and this may be a reason of decreasing apparent amount of consumed NO [32]. Only between 150 and 350°C NO consumption is significant and almost equal to NO_2 consumption in the case of 26%NO_2 in NO_x feed. Based on the knowledge of the “Fast SCR” [29] the following reactions can be proposed:

$$2NH_3 + H_2O \leftrightarrow 2NH_4^+ + O^{2-} \quad (7)$$

$$2NO_2 \leftrightarrow N_2O_4 \quad (8)$$

$$N_2O_4 + O^{2-} \leftrightarrow NO_2^- + NO_3^- \quad (9)$$

$$NO_2^- + NH_4^+ \leftrightarrow [NH_4NO_2] \rightarrow N_2 + 2H_2O \quad (10)$$

$$NO_3^- + NH_4^+ \leftrightarrow NH_4NO_3 \quad (11)$$

$$NH_4NO_3 \leftrightarrow N_2O + 2H_2O \quad (12)$$

$$NO + NO_3^- \leftrightarrow NO_2 + NO_2^- \quad (13)$$

According to the scheme, at temperatures higher than 150 °C reactions (7), (8), (9), (10), (11) take place yielding nitrogen and surface nitrate species. Disproportionation of adsorbed NO_2 (8), (9) was also suggested by DFT calculations earlier [33]. A small part of the surface nitrates is decomposed to N_2O (12), trace amount of which (< 5ppm) is observed in the reaction products at high temperatures. NO production from NO_2 (negative $NO_{converted}/NO_{2converted}$ ratio at T<150 °C on Fig.6) and the observation that the higher the NO_2 content – the larger is the part of NO_2 in the NO_x that is converted to N_2 in the NO/NO_2 experiments can be explained by reverse (13). NO reacts with surface nitrates according to (13) to form NO_2 and nitrite, which is readily decomposed to nitrogen (10). With that nitrates are partly removed from the catalyst surface and higher NO_x conversion is obtained.

With decreasing reaction temperature from 400 to 200 °C an increase in the NO_x conversion is observed. The effect is particularly evident for the 47% NO_2+NO mixture (Fig.5, solid curve) and may be due to the formation of surface NH_4NO_3. NH_4NO_3 formation is also consistent with decreased $NO_{converted}/NO_{2converted}$ ratio below 180 °C (Fig. 8) due to reaction stoichiometry:

$$2NH_3 + 2NO_2 \rightarrow NH_4NO_3 + N_2 + H_2O, \quad (14)$$

which is, in fact, a combination of (7) + (8) + (9) + (10) + (11), but without (12) and (13), which are too slow at this temperature. It is also rather indicative of NH_4NO_3 formation that below 200 °C we do not observe N_2O evolution, while above this temperature its decomposition (12) yields N_2O. Therefore, below 200 °C nitrate formation and subsequent blocking the alumina surface limits NO_x conversion.

To check the reaction scheme during an Al_2O_3 activity test, temperature ramping was stopped at 500, 210 and 100 °C. After the concentrations of the outlet gas components were stabilised, NH_3 was switched off from the feed. Following the removal of NH_3 from the inlet gas at 500 and 100 °C the concentrations of NO and NO_2 equalled these concentrations at the reactor inlet (no reaction with adsorbed nitrates (13) was observed). However, the removal of NH_3 from the feed at 210 °C (Fig. 9) resulted in consumption of NO and release of NO_2. This is in agreement with NO consumption in the NO_x SCR over alumina, which takes place between 150 and 350 °C (Fig. 8). The ratio of evolved NO_2 to consumed NO was approximately 1.7. This ratio can be achieved by combination of the competing reactions (10), which gives no NO_2, reverse (9) and (8), which give 2 NO_2 molecules, and, of course (13), which initiates the NO consumption and yields 1 NO_2 molecule. Thus the mechanism of NO_x SCR by NH_3 over Al_2O_3 and Ag/Al_2O_3 could share most of the reaction steps with "Fast SCR".

3.2.4 Surface species during NH_3-SCR over Al_2O_3

Diffuse reflectance infrared spectroscopy is a powerful tool to complement observations from catalytic experiments with observations of surface species. Fig. 10 shows the evolution of species on the Al_2O_3 surface, when switching off NH_3 from a feed containing NO, NO_2, NH_3 and O_2 at 150 °C and at 500 °C. Similar spectra were

observed at 300 and 400 °C but not shown. The first spectra are taken in a feed containing NH_3 and the following spectra 5, 10, 15 and 25 min after the NH_3 was switched off. When all gases are present in the first spectra, bands at 1690, 1623, 1533, 1474, 1398, 1314 and 1236 cm^{-1} can be distinguished at 150 °C. According to literature, the bands at 1623, 1533 and 1236 cm^{-1} which are accompanied by bands at 3355, 3271 and 3173 cm^{-1} (not shown) can be assigned to deformation vibrations and stretching vibrations of ammonia, respectively [34-37]. Bands at 1690 and 1474 cm^{-1} have previously been assigned to deformation vibrations of NH_4^+ or NH_3 [34, 35, 37]. At 500 °C all the bands are much smaller. But even there, mainly bands due to NH_3 or NH_4^+ can be observed. Thus under NH_3-SCR conditions, mainly ammonia is adsorbed on Al_3O_2 and very little nitrates and nitrites are adsorbed. When turning off ammonia in the feed first the bands of adsorbed NH_3 at 1236, 1623, 3355, 3271 and 3173 cm^{-1} decrease at 150 °C. Somewhat later, the NH_4^+ bands at 1690 and 1474 cm^{-1} start to decrease and two new bands at 1612 and 1585 cm^{-1} grow. At the same time, the bands around 1551 and 1308 cm^{-1} shift in wavenumber and increase. The shifts in wavenumber as well as the new bands are all caused by the stretching of the N=O bond of differently bound nitrate species [35-45] which start accumulating in the absence of NH_3. That the bands of adsorbed NH_3 diminish before the bands of adsorbed NH_4^+ species start to decrease is in accordance with reaction (14). Switching back to SCR reaction conditions, the NH_3 and NH_4^+ species start growing again at 150°C while the nitrate species decrease but do not completely disappear, even in the presence of H_2 as shown by the first spectra in Fig. 11.

At 500 °C, the bands of adsorbed NH_4^+ at 1690 and 1464 cm^{-1} disappear previous to the bands of adsorbed NH_3 between 3355 and 3173 cm^{-1} (not shown), while the nitrate

band at about 1551 cm^{-1} increases. The remaining nitrates may be regarded as inactive. However, whether the accumulation of these species reduce the activity for NO_x reduction and, thus, poison the surface or only act as spectator species, cannot be answered by the available data.

Fig. 11 shows, moreover, the evolution of bands when switching off NH_3 from a H_2 containing feed at different temperatures. At all temperatures, the spectra are dominated by nitrates with bands at 1551, around 1585, 1612 and around 1304 cm^{-1}. The amount of adsorbed species decreases with increasing temperature as indicated by fewer and smaller peaks at higher temperatures. When the ammonia is switched off from the feed containing H_2 at 150°C the bands assigned to NH_3 and NH_4^+ species on the surface decrease while the nitrate bands around 1615, 1585, 1551 and 1301 cm^{-1} increase. This evolution of the bands is similar to the case without H_2 in the feed. At 300 °C, only the nitrate band at 1585 cm^{-1} increase, while the other nitrate bands are stable or decrease. At even higher temperatures, all NH_x bands are very tiny or hardly visible while all nitrate bands clearly decrease showing that the addition of H_2 to the feed has an influence on γ-Al_2O_3 without silver. For this observed effect of hydrogen at high temperatures (400 and 500 °C) there are two reasonable explanations: hydrogen may either itself reduce the nitrates as observed by [26, 31, 46] on Ag/Al_2O_3 or it partially reduces some of the NO_2 to NO which in turn can reduce nitrates to nitrites (reaction 13). Moreover, less new nitrates will be formed on the catalyst surface when the NO_2 concentration is decreased by partial reduction to NO.

3.3. DFT calculations

3.3.1. Oxidation of NO to NO_2 and NO_3 on the surface of transition metals

Figure 12 shows the potential energy surface diagram for the absorption of NO and O_2 leading to NO_x, i.e. NO_2 and NO_3 calculated for 6 different transition metal catalysts Ag, Cu, Pd, Pt, Rh and Ru. For all six different transition metal catalysts both the (111) terrace surface model and (211) step surface model were investigated and the results are similar for both surfaces. The diagram shows that among the transition metals studied the formation of NO_2 on (111) terraces is favorable for both Ag and Cu, whereas the formation of NO_3 is favorable only on Ag. On (211) step surface the formation of NO_2 and NO_3 via oxidation of NO is significantly favorable only on Ag. For other metals NO adsorption without oxidation to NO_x is preferred. That supports the idea of Ag being necessary catalyst component for the oxidation of NO to NO_x species as potentially first step of NO SCR.

3.3.2. Adsorption of NO_x and HNO_x on the step γ-Al_2O_3 surface

The model of the step on the γ-Al_2O_3 (representing uncoordinated Al sites) was used for calculations of NO_x adsorption energy as the most abundant surface of γ-Al_2O_3 crystals is the step surface [24]. It has been demonstrated by Donghai Mei et al. [33] that NO_3 adsorbs rather strongly on the γ-Al_2O_3 (100) and γ-Al_2O_3 (110) surfaces than compared to NO and NO_2.

A clear decrease of concentration of surface nitrates has been observed by FTIR after addition of hydrogen at high temperatures (experiments at 400 and 500 °C in the section 3.2.4). Such removal of strongly bound nitrates which block the alumina surface can partly explain the positive effect of H_2 on the activity of Ag/Al_2O_3 catalysts in NO_x SCR.

Though authors of [33] have done extensive calculation for the adsorption of NO_x on γ-Al_2O_3 (100) and γ-Al_2O_3 (110) surfaces, however no effect of H_2 on the stability of surface nitrates on γ-Al_2O_3 has been considered.

We have calculated the adsorption energy of NO_3 and HNO_3 on our model γ-Al_2O_3 step surface representing uncoordinated Al surface sites. Five different uncoordinated Al sites are present in our model alumina surface as derived from the bulk γ-Al_2O_3 geometry in [24]. These have all been used for the calculations, however only the most energetically favorable (energy minimum among studied) adsorption geometries with two oxygen atoms of NO_3 and HNO_3 bridging with two Al sites of γ-Al_2O_3 are reported here. See supplementary information for more details on the used geometries.

The calculated adsorption energy of HNO_3 (Fig. 13) on the model surface of γ-alumina is considerably smaller than that of NO_3 (which agrees with [33]), which increases the probability of HNO_3 removal from the alumina surface compared to NO_3 in the absence of hydrogen. This supports the suggestion of H_2 facilitating removal of strongly bound NO_3 from the alumina.

The mechanism of reduction of adsorbed NO_x species by hydrogen with the formation of N_2 has been previously suggested for Pt/MgO-CeO_2 catalysts for H_2-SCR of NO_x [20, 21]. This mechanism includes dissociative adsorption of hydrogen on the metal nanoparticle, spillover of the formed atomic hydrogen on the support to the two neighboring NO_x species and their reduction with subsequent release of surface sites. However, this is not a major pathway of the SCR in our case because SCR in the absence of NH_3 is insignificant (Fig. 3, dotted line). Here we suggest that atomic hydrogen reacts rather with a single nitrate or nitrite group with subsequent release of

HNO_x and adsorption sites on alumina. The evolved HNO_x can recombine with the formation of water and nitrogen oxides.

4. Conclusions

Ag supported on γ-Al_2O_3 is a very promising catalytic system which can be used for the removal of nitrogen oxides from the exhaust of diesel engines in the presence of H_2. It is vital that both Ag and alumina are present in the catalyst formulation. The primary role of Ag is the H_2-assisted oxidative activation of NO and the reaction of oxidized NO and NH_3 can proceed further on alumina. Hydrogen also facilitates removal of nitrates from the alumina surface, as supported by DRIFTS experiments and DFT calculation.

The studied catalysts facilitate NO+NO_2 mixture reduction without H_2 in the feed with the Al_2O_3 support defining the catalytic activity. Therefore, tuning the alumina support, not only the metal, is vital for obtaining active Ag/Al_2O_3 catalyst.

5. Acknowledgments

This work was supported by grant 09-067233 from The Danish Council for Strategic Research. TEM images were acquired with the support of Center for Electron Nanoscopy (DTU CEN) and personally by Thomas W. Hansen. We acknowledge the supply of the commercial alumina for the study by the SASOL Germany .

The authors also wish to thank Dr. Alexander Yu. Stakheev and Dr. Jakob Weiland Høj for fruitful discussions.

References

[1] T.V. Johnson, Int. J. Engine Res. 10 (2009) 275-285

[2] S. Subramanian, R.J. Kudla, W. Chun, M. Chatth, Ind. Eng. Chem. Res. 32 (1993) 1805-1810

[3] T. Miyadera, Appl. Catal. B 2 (1993)199-205

[4] G.E. Marnellos, E.A. Efthimiadis, I.A. Vasalos, Appl. Catal. B 48 (2004) 1-15

[5] Z.M. Liu, K.S. Oh, S.I. Woo, Catal. Lett. 106 (2006) 35-40

[6] S. Satokawa, J. Shibata, K. Shimizu, S. Atsushi, T. Hattori, Appl. Catal. B 42 (2003) 179-186

[7] R. Burch, J.P. Breen, C.J. Hill, B. Krutzsch, B. Konrad, E. Jobson, L. Cider, K. Eranen, F. Klingstedt, L.E. Lindfors, Top. Catal. 30-31 (2004) 19-25

[8] M. Richter, U. Bentrup, R. Eckelt, M. Schneider, M.M. Pohl, R. Fricke, Appl. Catal. B 51 (2004): 261-274

[9] M. Richter, R. Fricke, and R. Eckelt, Catal. Lett. 94 (2004) 115-118

[10] K.-i. Shimizu, and A. Satsuma, Appl. Catal. B 77 (2007) 202-205

[11] H. Kannisto, X. Karatzas, J. Edvardsson, L.J. Pettersson, H.H. Ingelsten, Appl. Catal. B 104 (2011) 74-83

[12] S. Bensaid, E.M. Borla, N. Russo, D. Fino, V. Specchia, Ind. Eng. Chem. Res. 49 (2010) 10323–10333

[13] T. Johannessen, H. Schmidt, US patent 2010/0021780 A1

[14] C.H. Christensen, R.Z. Sørensen, T. Johannessen, U.J. Quaade, K. Honkala, T.D. Elmøe, R. Køhler, J.K. Nørskov, J. Mater. Chem. 15 (2005) 4106-4108

[15] A. Klerke, C.H. Christensen, J.K. Nørskov, T. Vegge, J. Mater. Chem. 18 (2008) 2304-2310

[16] V.A. Kondratenko, U. Bentrup, M. Richter, T. W. Hansen, and E. V. Kondratenko, Appl. Catal. B 84 (2008) 497-504

[17] K.-i. Shimizu, and A. Satsuma, J. Phys. Chem. C 111 (2007) 2259-2264

[18] E. Kondratenko, V. Kondratenko, M. Richter, and R. Fricke, J. Catal. 239 (2006) 23-33

[19] P.G. Savva, C.N. Costa, Catal. Rev. - Sci. Eng., 53 (2011) 91-151

[20] C.N. Costa, A.M. Efstathiou, J. Phys. Chem. C111 (2007) 3010-3020

[21] P.G. Savva, A.M. Efstathiou, J. Catal. 257 (2008) 324–333

[22] E. Mènendez-Proupin, G. Gutièrrez, Phys. ReV. B 72 (2005) 35116-35119

[23] B. Hammer, L.B. Hansen, J.K. Nørskov, Phys. ReV. B 59 (1999) 7413–7421

[24] M. Digne, P. Sautet, P. Raybaud, P. Euzen, H. Toulhoat, J. Catal. 226 (2004) 54–68

[25] P. Sazama, L. Čapek, H. Drobná, Z. Sobalík, J. Dědeček, K. Arve, B. Wichterlová, J. Catal. 232 (2005) 302-317

[26] K.-i. Shimizu, J. Shibata, A. Satsuma, J. Catal. 239 (2006) 402-409

[27] V. Houel, P. Millington, R. Rajaram, A. Tsolakis, Appl. Catal. B 77 (2007) 29-34

[28] G. Madia, M. Koebel, M. Elsener, A. Wokaun, Ind. Eng. Chem. Res. 41 (2002) 3512-3517

[29] A. Grossale, I. Nova, E. Tronconi, D. Chatterjee, M. Weibel, J. Catal. 256 (2008) 312-322

[30] J.H. Lee, S.J. Schmieg, S.H. Oh, Appl. Catal. A 342 (2008) 78-86

[31] F.C. Meunier, J. Ross, Appl. Catal. B 24 (2000) 23-32

[32] J.G.M. Brandin, L.H. Andersson, C.U.I. Odenbrand, Acta Chemica Scandinavica 44 (1990) 784-788

[33] D. Mei, Q. Ge, J. Szanyi, and C.H.F. Peden, J. Phys. Chem. C 113 (2009) 7779–7789

[34] A.A. Tsyganenko, D.V. Pozdnyakov, V.N. Filimonov, J. Mol. Struct. 29 (1975) 299-318

[35] J.B. Peri, J. Phys. Chem. 69 (1965) 231-239

[36] A.A. Davydov, Infrared spectroscopy of adsorbed species on the surface of transition metal oxides, John Wiley & Sons, Chichester, New York, Brisbane, Toronto, Singapore, 1984

[37] G. Busca, H. Saussey, O. Saur, J.C. Lavalley, V. Lorenzelli, Appl. Catal. 14 (1985) 245-260

[38] A. Iglesias-Juez, A.B. Hungria, A. Martinez-Arias, A. Fuerte, M. Fernandez-Garcia, J.A. Anderson, J.C. Conesa, J. Soria, J. Catal. 217 (2003) 310-323

[39] S. Tamm, H.H. Ingelsten, M. Skoglundh, A.E.C. Palmqvist, J. Catal. 276 (2010) 402-411

[40] S. Tamm, H.H. Ingelsten, A.E.C. Palmqvist, J. Catal. 255 (2008) 304-312

[41] S. Kameoka, Y. Ukisu, T. Miyadera, Phys. Chem. Chem. Phys. 2 (2000) 367-372

[42] F.C. Meunier, J.P. Breen, V. Zuzaniuk, M. Olsson, J.R.H. Ross, J. Catal. 187 (1999) 493-505

[43] K.I. Hadjiivanov, Catal. Rev. Sci. Eng. 42 (2000) 71-144

[44] G.G. Ramis, G. Busca, V. Lorenzelli, P. Forzatti, Appl. Catal. 64 (1990) 243-257

[45] M. Schraml-Marth, A. Wokaun, A. Baiker, J. Catal. 138 (1992) 306-321

[46] H. Kannisto, H.H. Ingelsten, M. Skoglundh, Top. Catal. 52 (2009) 1817-1820

Figure legends

Figure 1. NO_x conversion profiles obtained over Ag/Al_2O_3, Ag/TiO_2, and In/Al_2O_3. Reaction conditions: 500 ppm NO, 520 ppm NH_3, 1200 ppm H_2, 8.3% O_2, 7% H_2O in Ar, GHSV = 110 000 h^{-1}.

Figure 2. TEM images of Ag/Al_2O_3 (left) and Ag/TiO_2 (right) calcined at 550°C in air.

Figure 3. NO conversion to NO_2 (solid line) and NO_x conversion to N_2 (dotted line) over Ag/Al_2O_3 without ammonia in the feed. Reaction conditions: 500 ppm NO, 1200 ppm H_2, 8.3% O_2, 7% H_2O in Ar, GHSV = 110 000 h^{-1}.

Figure 4. Total NH_3 conversion (solid line) and NH_3 conversion to NO_x (dotted line) over Ag/Al_2O_3 with no NO in the feed. Reaction conditions: 520 ppm NH_3, 1200 ppm H_2, 8.3% O_2, 7% H_2O in Ar, GHSV = 110 000 h^{-1}.

Figure 5. NO_x conversion over Ag/Al_2O_3 and Ag/ZrO_2 without H_2 in the feed, when NO and NO_2 mixture is fed as NO_x (NO_2 content is specified, NO is the rest of 500 ppm NO_x). Conditions: 500 ppm NO_x, 520 ppm NH_3, 8.3% O_2, 7% H_2O in Ar, GHSV = 110 000 h^{-1}.

Figure 6. Ratio of consumed NO to consumed NO_2 for simultaneous NO + NO_2 reduction by NH_3 over Ag/Al_2O_3. Reaction conditions: 500 ppm NO_x (NO_2 fraction is stated near the corresponding curves), 520 ppm NH_3, 8.3% O_2, 7% H_2O in Ar, GHSV = 110 000 h^{-1}.

Figure 7. NO_x conversion over Al_2O_3 (solid line) and Ag/Al_2O_3 (dotted line, for a comparison) without H_2 in the feed, when NO and NO_2 mixture is fed as NO_x. Reaction conditions: 500 ppm NO_x (37% NO_2), 520 ppm NH_3, 8.3% O_2, 7% H_2O in Ar, GHSV = 110 000 h^{-1}.

Figure 8. Ratio of consumed NO to consumed NO_2 for NO + NO_2 simultaneous reduction by NH_3 over Al_2O_3 (solid line) and Ag/Al_2O_3 (dotted line, for a comparison). Reaction conditions: 500 ppm NO_x (26% NO_2), 520 ppm NH_3, 8.3% O_2, 7% H_2O in Ar, GHSV = 110 000 h^{-1}.

Figure 9. Change of NO, NO_2 and NO_x concentrations after removing NH_3 from the feed. Catalyst: Al_2O_3. Reaction conditions: 500 ppm NO_x (37% NO_2), 520 ppm NH_3, 8.3% O_2, 7% H_2O in Ar, GHSV = 110 000 h^{-1}, temperature 210°C.

Figure 10. Change in surface species after removing NH_3 for the first time from the feed over a fresh Al_2O_3 catalyst. Reaction conditions: 500 ppm NO_x (37% NO_2), 520 ppm NH_3, 8.3% O_2 in Ar. Spectra were taken from gray to black: with NH_3 in the feed, and 5, 10, 15 and 25 min after switching off NH_3.

Figure 11. Change in surface species after removing NH_3 from the hydrogen-containing feed over Al_2O_3. Reaction conditions: 500 ppm NO_x (37% NO_2), 520 ppm NH_3, 1250 ppm H_2, 8.3% O_2 in Ar. Spectra were taken from gray to black: with NH_3 in the feed, and 5, 10, 15 and 25 min after switching off NH_3.

Figure 12. Potential energy surface diagram for the formation of NO_x via the oxidation of NO over (111) and (211) surfaces of the selected transition metals.

Figure 13. NO_3 and HNO_3 adsorption geometries and adsorption energies on the model step closed packed gamma alumina surface. All the adsorption energies are given with the reference to the gas phase zero energy points of the respective species.

Table 1

Catalyst	Metal loading, wt%	Support BET surface area, m^2/g	NO_x conversion	
			0 ppm H_2	1200 ppm H_2
Al_2O_3	-	140	0	0
Ag/Al_2O_3	1	140	0	94
Ag/TiO_2	1	110	1.5	25
Ag/ZrO_2	1	14	0	0
Sn/Al_2O_3	3	140	0	0
In/Al_2O_3	3	140	0	10.5

Table 1. Studied catalysts and NO_x conversions obtained at 380°C without and with H_2 in the feed gas. Reaction conditions: 500 ppm NO, 520 ppm NH_3, 8.3% O_2, 7% H_2O in Ar, GHSV = 110 000 h^{-1}.

Figure 1 revised

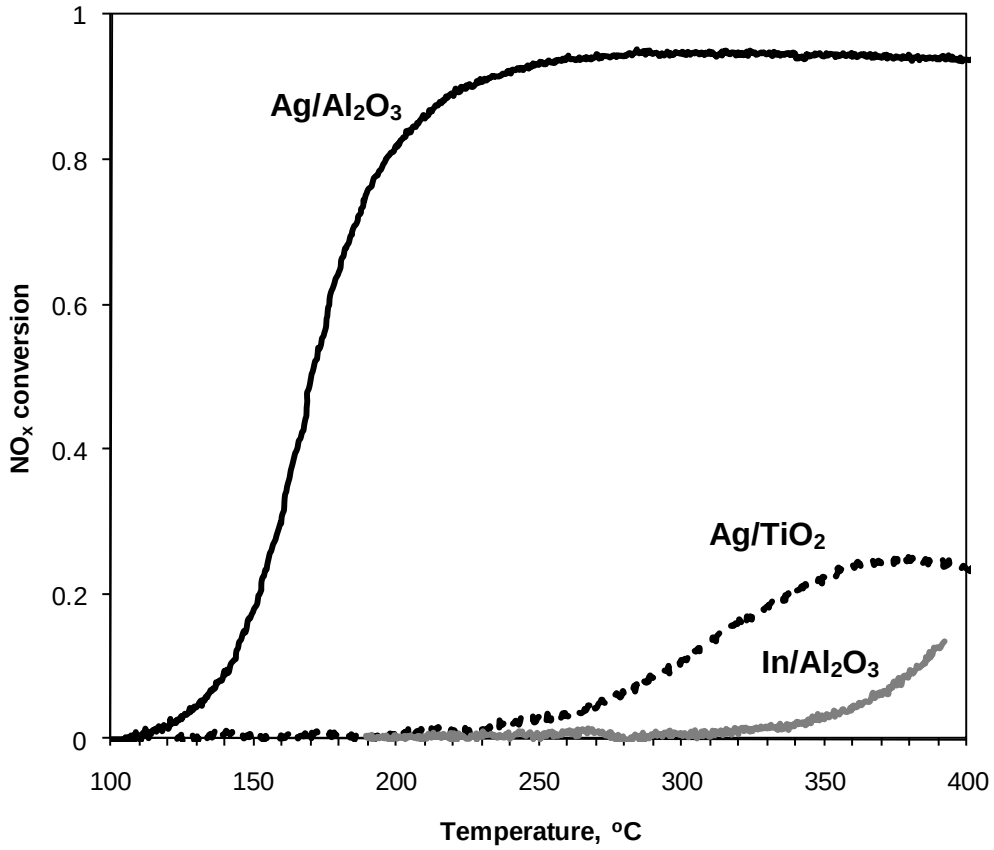

Figure 2

Click here to download high resolution image

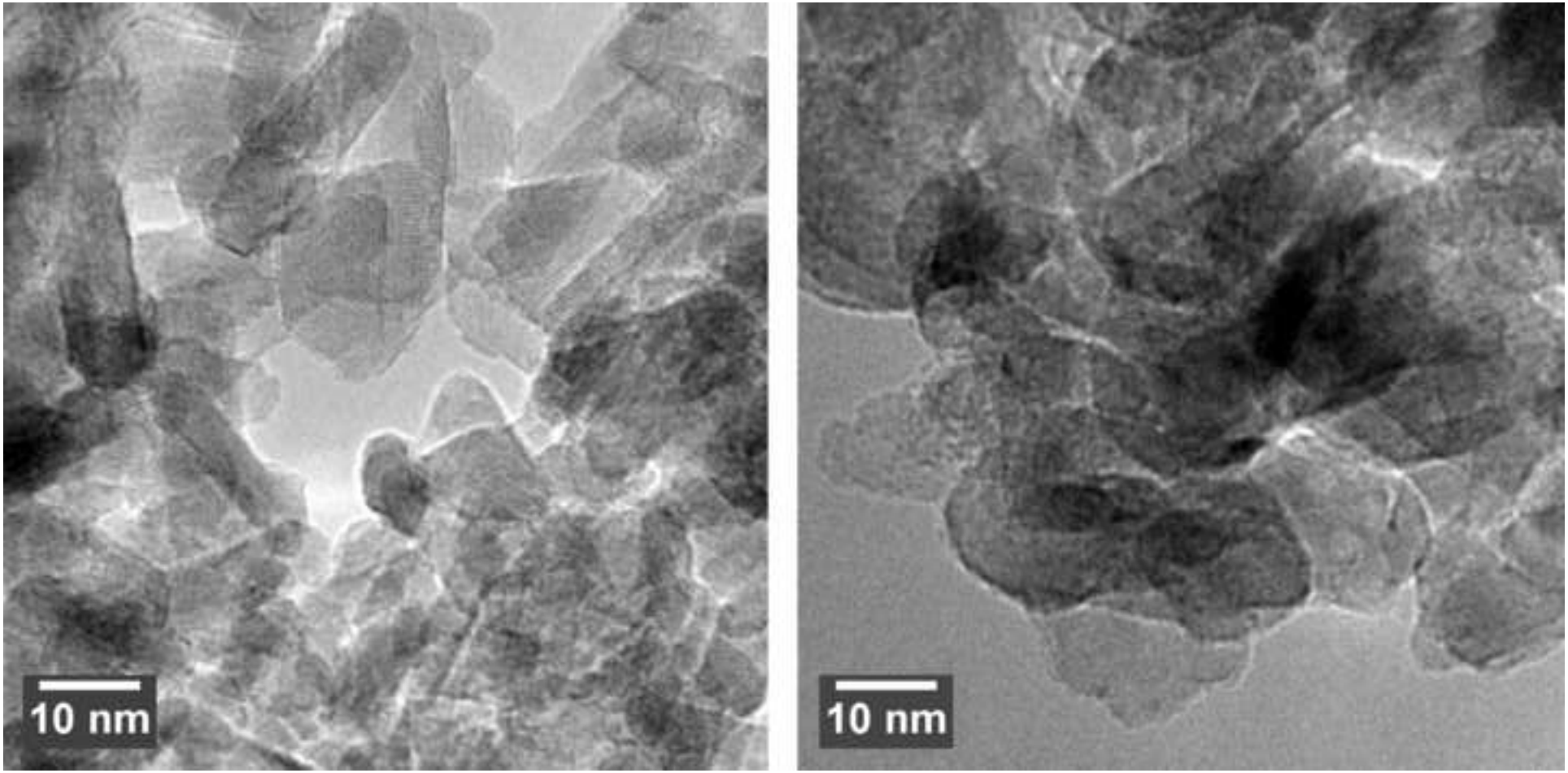

Figure 3 revised

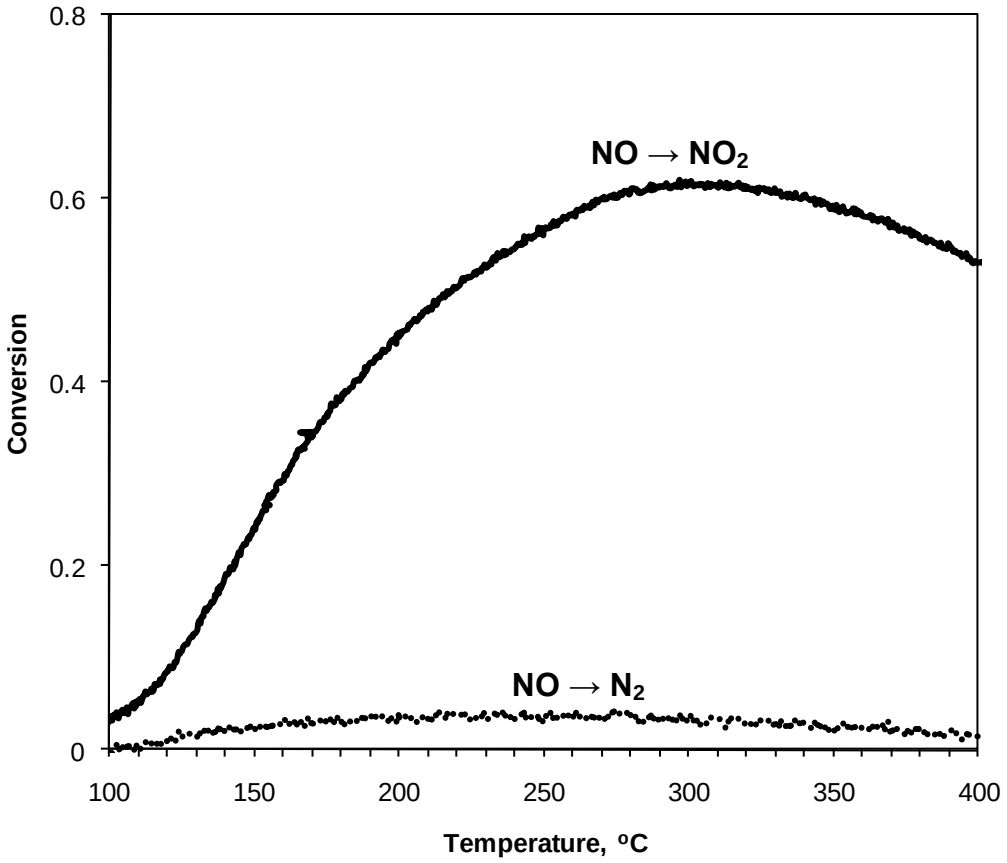

Figure 4 revised

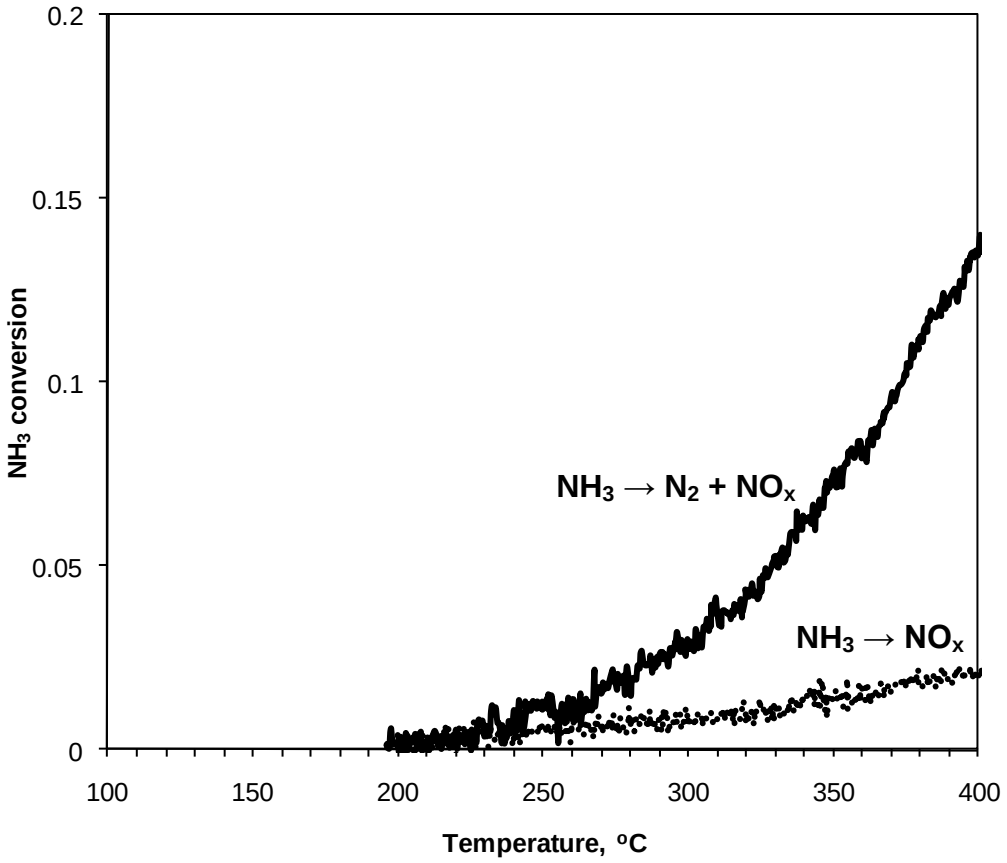

Figure 5 revised

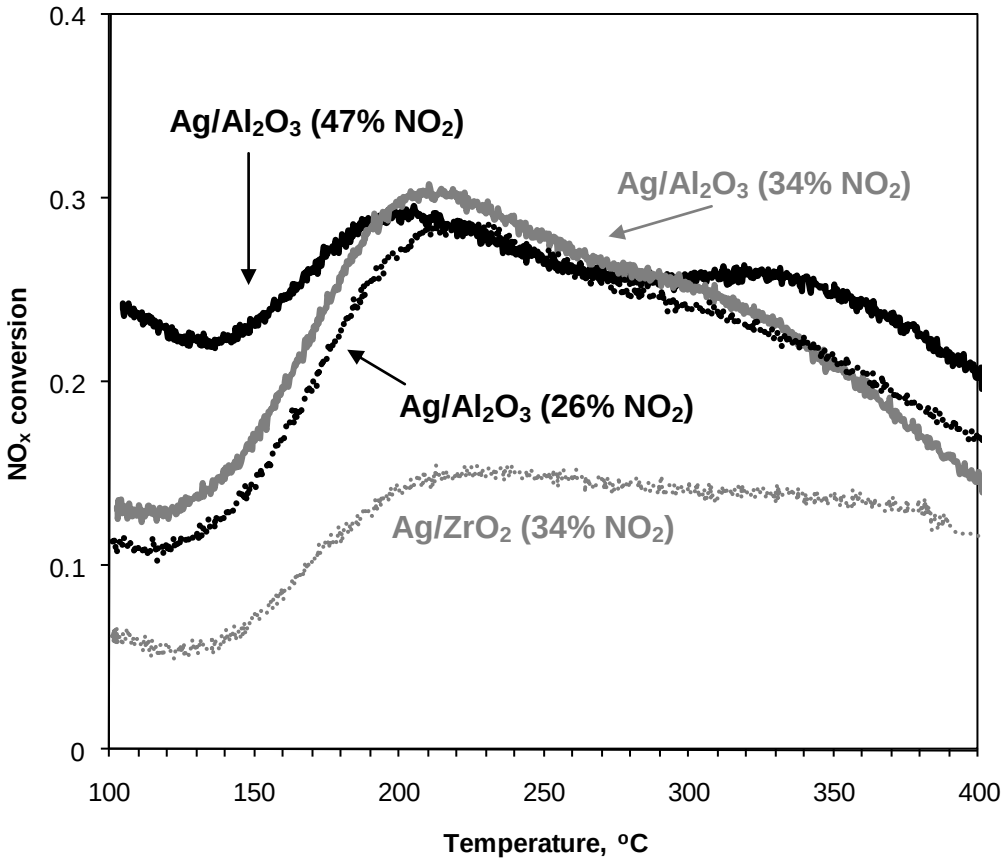

Figure 6 revised

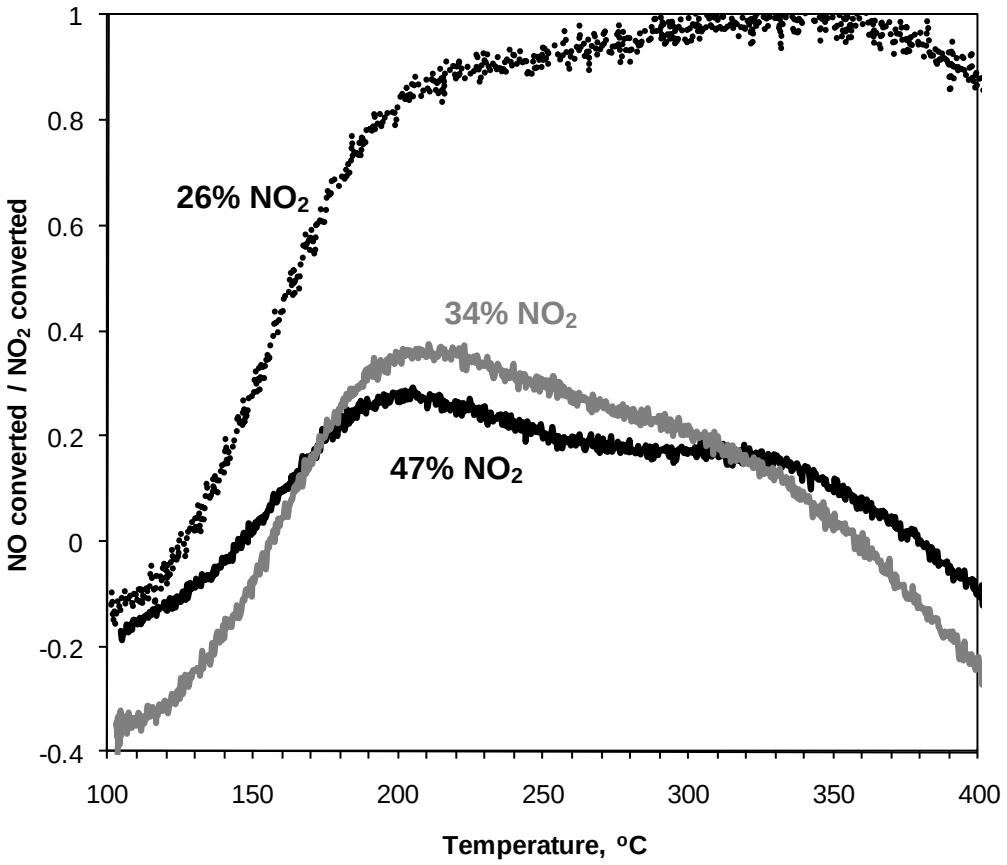

Figure 7 revised

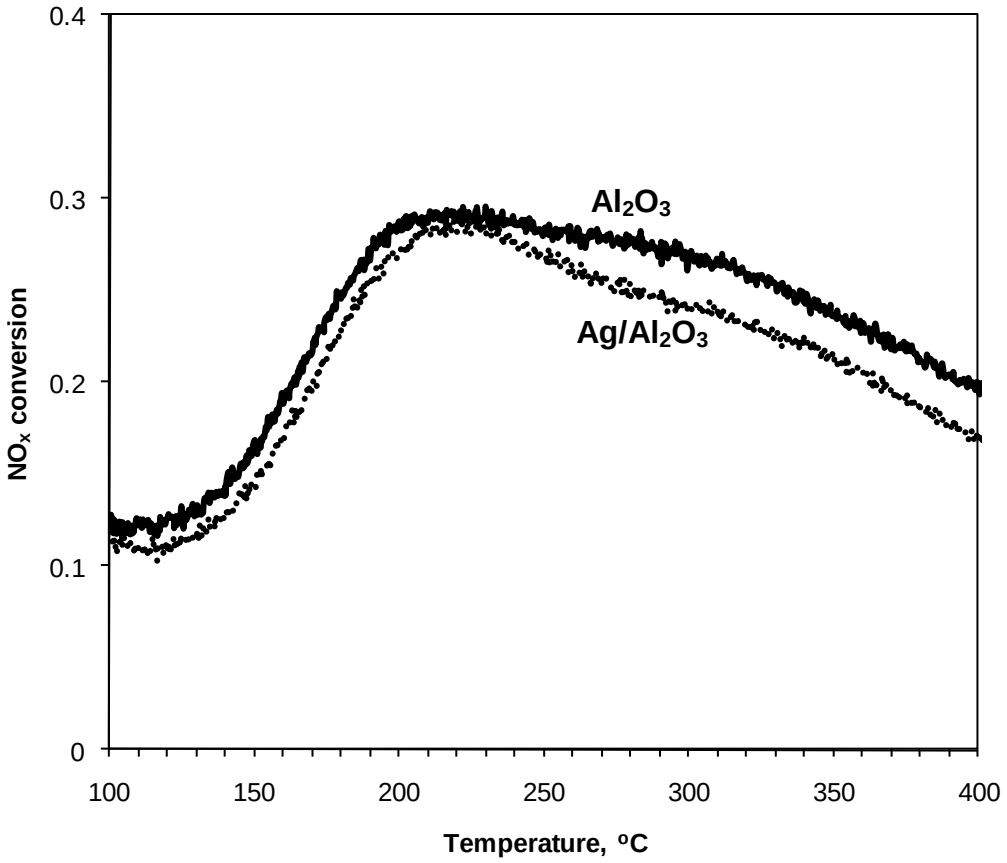

Figure 8 revised

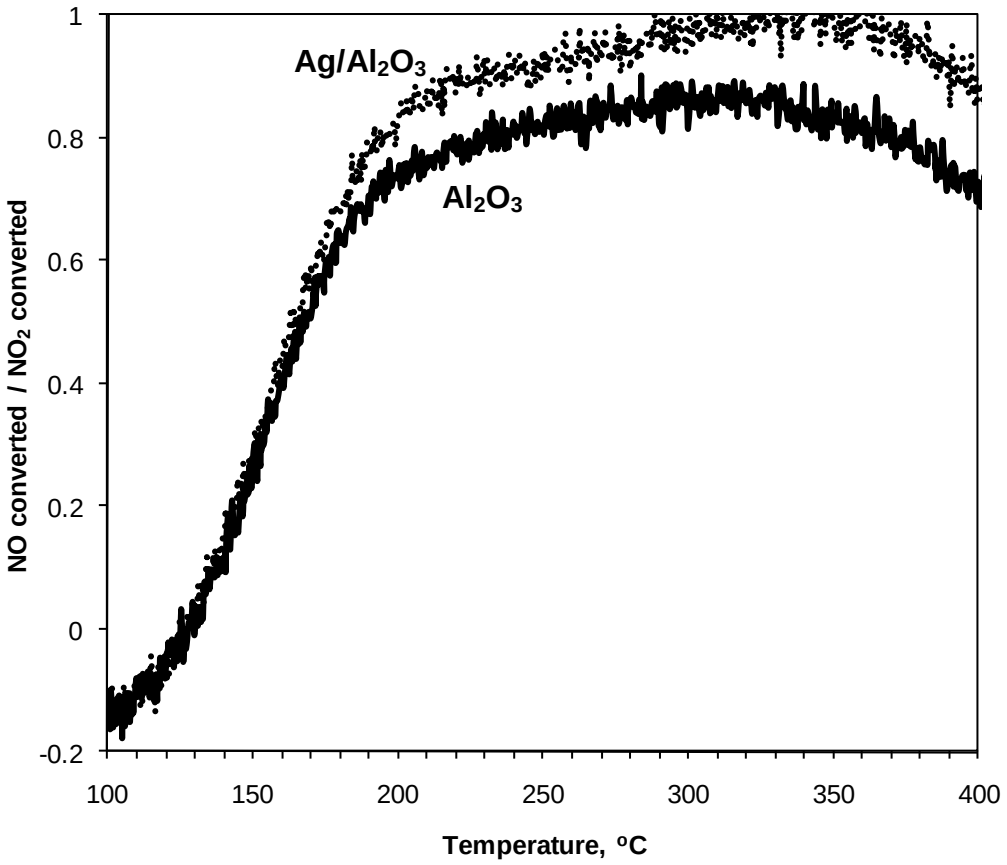

Figure 9 revised

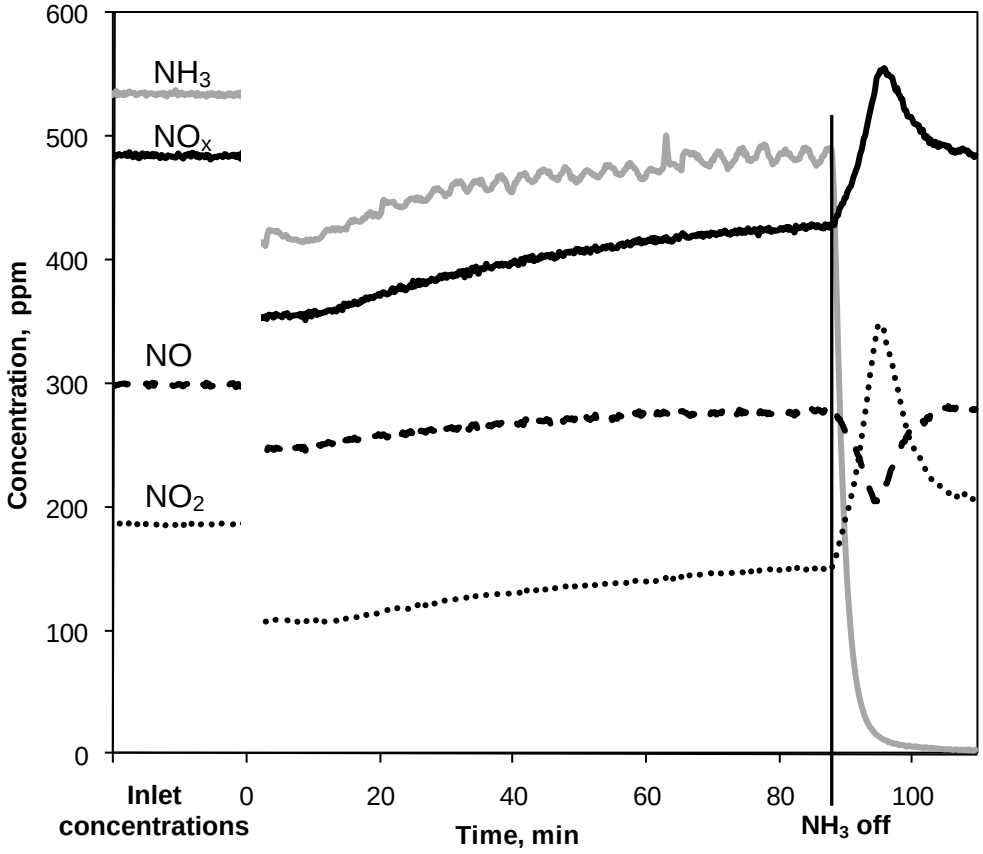

Figure 10 revised

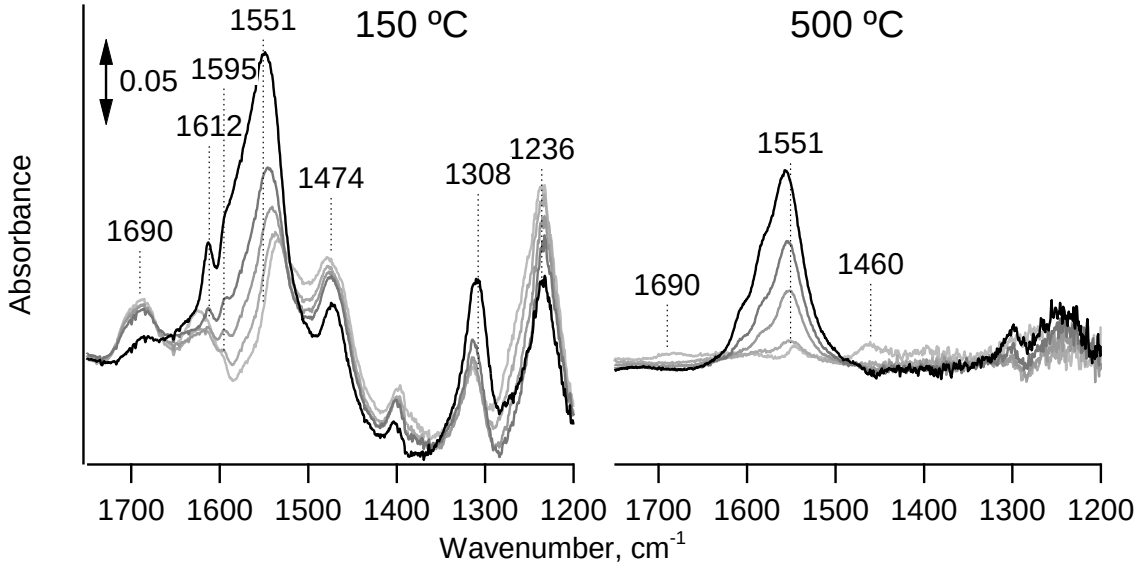

Figure 11 revised

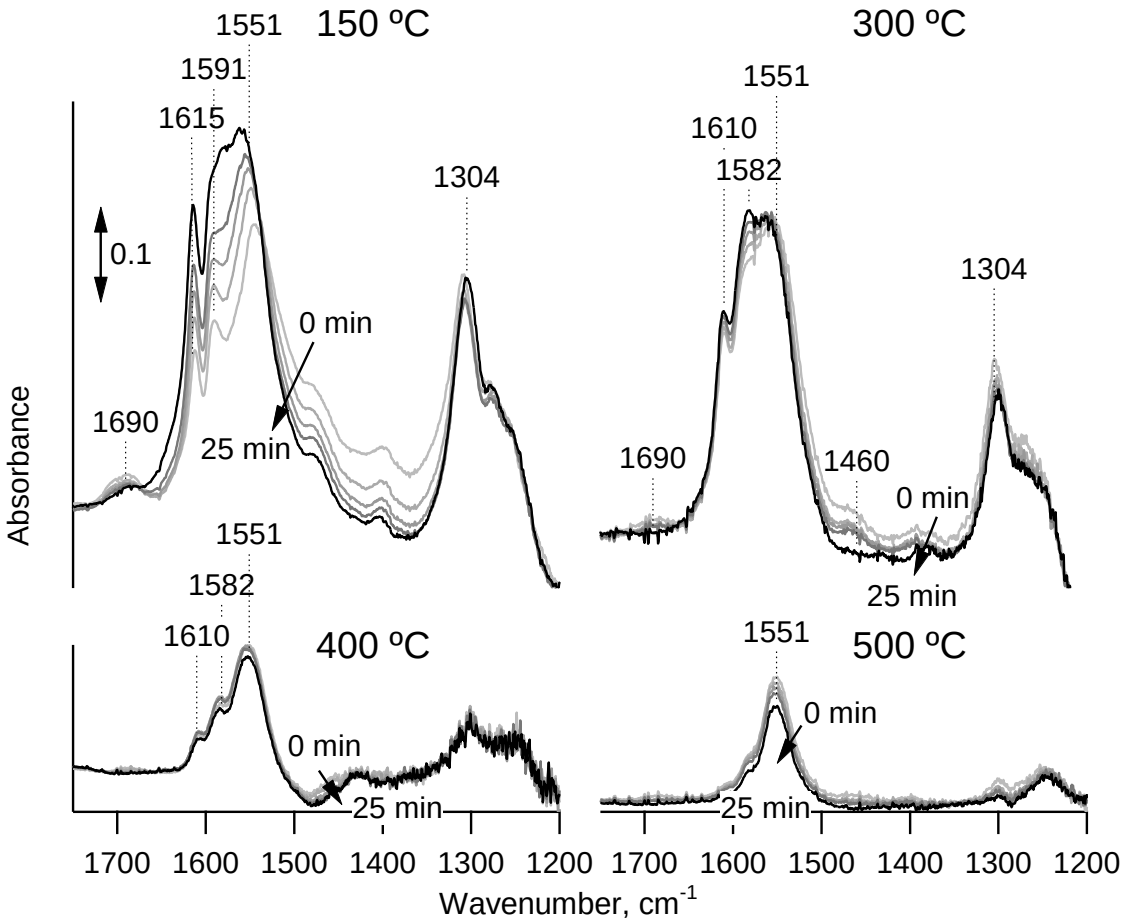

Figure 12 color for web

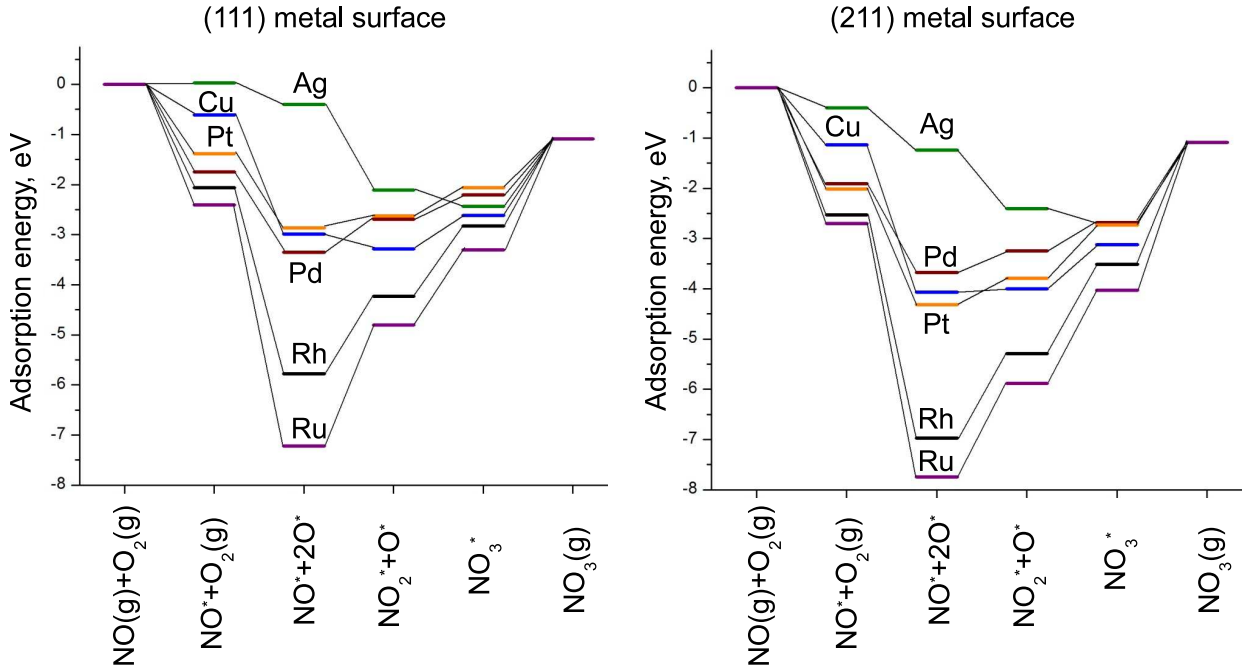

Figure 12 grayscale for print

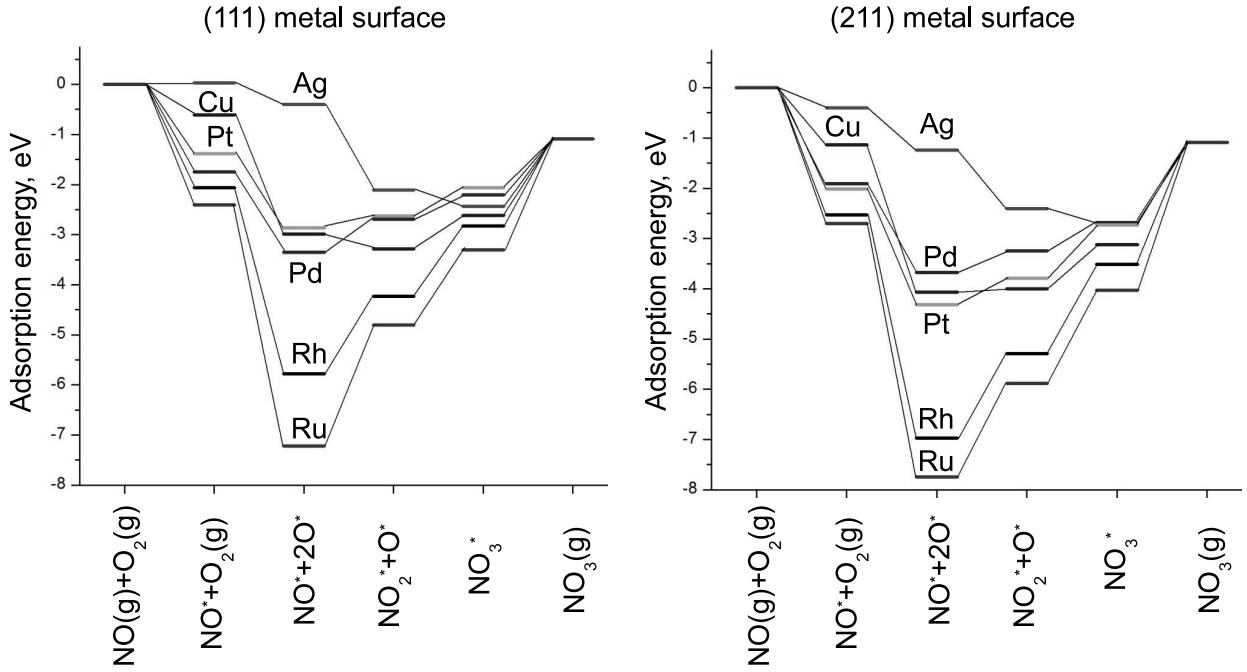

Figure 13 color for web

Click here to download high resolution image

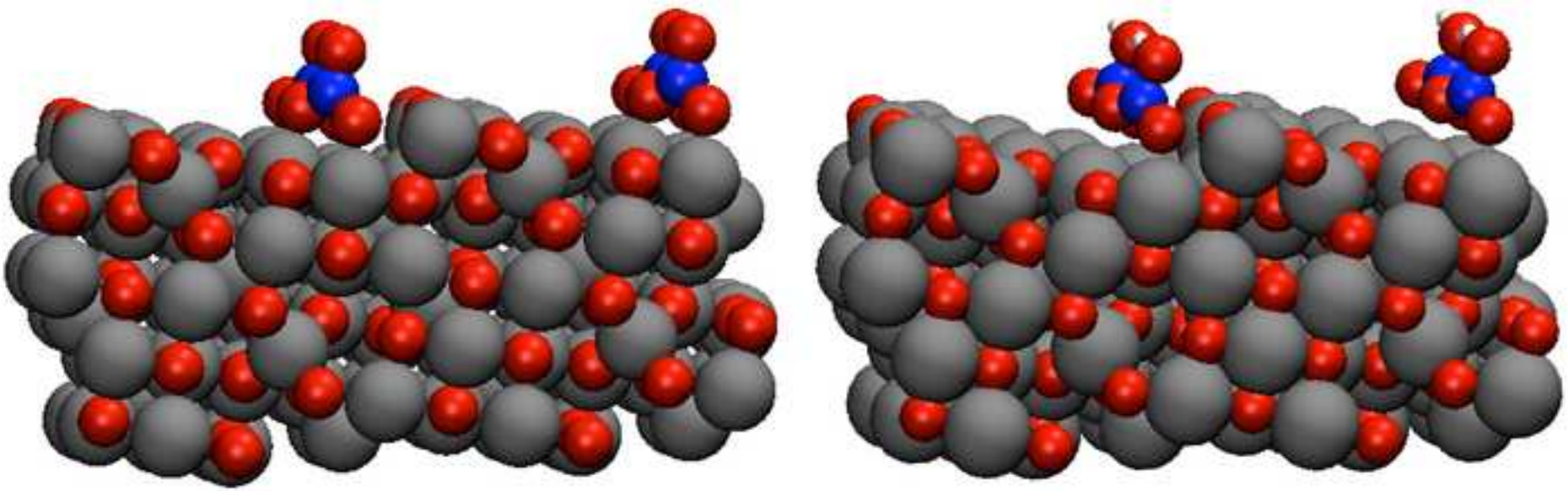

Figure 13 grayscale for print

Click here to download high resolution image